PHYSICS OF FLUIDS **25**, 122002 (2013)

Thermodiffusion in concentrated ferrofluids: A review and current experimental and numerical results on non-magnetic thermodiffusion

Lisa Sprenger,[a] Adrian Lange, and Stefan Odenbach
Institute of Fluid Mechanics, Chair of Magnetofluiddynamics, Measuring and Automation Technology, TU Dresden, 01062 Dresden, Germany

(Received 20 June 2013; accepted 7 November 2013; published online 20 December 2013)

Ferrofluids are colloidal suspensions consisting of magnetic nanoparticles dispersed in a carrier liquid. Their thermodiffusive behaviour is rather strong compared to molecular binary mixtures, leading to a Soret coefficient (S_T) of $0.16\,K^{-1}$. Former experiments with dilute magnetic fluids have been done with thermogravitational columns or horizontal thermodiffusion cells by different research groups. Considering the horizontal thermodiffusion cell, a former analytical approach has been used to solve the phenomenological diffusion equation in one dimension assuming a constant concentration gradient over the cell's height. The current experimental work is based on the horizontal separation cell and emphasises the comparison of the concentration development in different concentrated magnetic fluids and at different temperature gradients. The ferrofluid investigated is the kerosene-based EMG905 (Ferrotec) to be compared with the APG513A (Ferrotec), both containing magnetite nanoparticles. The experiments prove that the separation process linearly depends on the temperature gradient and that a constant concentration gradient develops in the setup due to the separation. Analytical one dimensional and numerical three dimensional approaches to solve the diffusion equation are derived to be compared with the solution used so far for dilute fluids to see if formerly made assumptions also hold for higher concentrated fluids. Both, the analytical and numerical solutions, either in a phenomenological or a thermodynamic description, are able to reproduce the separation signal gained from the experiments. The Soret coefficient can then be determined to $0.184\,K^{-1}$ in the analytical case and $0.29\,K^{-1}$ in the numerical case. Former theoretical approaches for dilute magnetic fluids underestimate the strength of the separation in the case of a concentrated ferrofluid. © *2013 AIP Publishing LLC*. [http://dx.doi.org/10.1063/1.4848656]

I. INTRODUCTION

A magnetic fluid, also called ferrofluid, consists of magnetic nanoparticles with a diameter of approximately 10 nm which are dispersed in a carrier liquid. To guarantee a stericly stable dispersion of the particles in the fluid they are coated with a layer of surfactant with a thickness of approximately 2 nm. The magnetic material usually used for the particles is magnetite (Fe_3O_4) or cobalt (Co), the carrier is often kerosene-, oil-, or water-based.[1,2] In the context of thermally driven transport processes the ferrofluid is mainly characterised by the particle diameter, the diameter's size distribution, the particles' volume concentration, and the dynamic viscosity.

Thermal diffusion, also called thermodiffusion or Ludwig-Soret-effect, denotes a transport process in a finite volume of a binary fluid exposed to a temperature gradient.[3] The fluid layer demixes under the influence of the temperature difference at its boundaries. In the case of colloidal suspensions, the demixing refers to the movement of the particles to one boundary of the layer.[4–6] The intensity and direction of the transport is thereby characterised by the Soret coefficient (S_T). A positive

[a] Author to whom correspondence should be addressed. Electronic mail: Lisa.Sprenger@tu-dresden.de

(negative) coefficient drives the particles to the colder (hotter) part of the fluid cell.[6] Thermodiffusion was first observed in fluid mixtures[7,8] but is far more intense in colloidal suspensions. The Soret coefficient of ferrofluids ($S_T \approx 0.16\ \mathrm{K}^{-1}$)[4,9] differs by approximately two orders of magnitude from the one measured in fluid mixtures such as n-hexane/toluene or dodecane/1,2,3,4-tetrahydronaphthalene where the values for S_T vary between $0.003\ \mathrm{K}^{-1}$ and $0.009\ \mathrm{K}^{-1}$.[10,11]

Since magnetic fluids are often used as thermal conductors, e.g., in loudspeaker technology,[2,12] and are therefore exposed to temperature gradients, the separation process due to thermodiffusion has a direct impact on the application. An arising concentration gradient leads to gradients in other thermophysical fluid parameters such as viscosity, magnetisation, or conductivity.[1,13,14] Therefore, beside from the point of the basic research, a better and deeper understanding of thermodiffusion especially in concentrated magnetic fluids is desirable.

II. REVIEW ON THERMODIFFUSION—THEORY AND MEASUREMENT

Different research groups during the last 20 years dedicated their work to the investigation of thermal diffusion mainly in dilute ferrofluids.[9,15–18] There were three different main setups used for the experimental part. First, the forced Rayleigh scattering (FRS) by Bacri *et al.*[15] and Lenglet *et al.*,[16] then several experiments using a vertical thermodiffusion cell by Blums *et al.*[17] and Völker *et al.*,[9] and finally the horizontal thermodiffusion cell also used by Völker and Odenbach.[18] The principle of the diffusion cell is to apply a temperature difference to a gap filled with a magnetic fluid, which then separates under the effect of the temperature gradient. The fluid's particles and the carrier liquid move to different directions into separated fluid reservoirs where the corresponding species will become enriched. To monitor the separation process the particles' volume concentration is detected by sensor coils wrapped around the reservoirs. In the case of the vertical diffusion cell the gap is positioned vertically, the concentration and the resulting fluid's density gradient establish perpendicular to the gap and therefore buoyancy-driven convection arises and enhances the separation process. The horizontal thermodiffusion cell is characterised by a horizontally placed fluid gap. The direction of the applied temperature gradient is then chosen to establish a stable density layering to avoid convection processes. Due to this advantage this setup is chosen for the investigations of this work.

Thermal diffusion can mathematically be described either by the phenomenological diffusion equation[3] or by the ferrofluiddynamics-theory (FFD-theory).[19,20] The diffusive mass transport in the first case[3]

$$\frac{\vec{j}}{\rho} = -D\left[\vec{\nabla}c + S_T c(1-c)\vec{\nabla}T\right] \tag{1}$$

consists of the molecular diffusion driven by a concentration gradient $\vec{\nabla}c$ and thermal diffusion driven by a temperature gradient $\vec{\nabla}T$ with $\vec{j}$ denoting the mass transport of the fluid's particles, D the diffusion coefficient, S_T the Soret coefficient, T the temperature, $c = \frac{\rho_1}{\rho}$ the mass concentration of the particles, and $\rho = \sum_{i=1}^{N} \rho_i$ the total density as sum of the components' densities ρ_i. In the case of a dilute fluid it is assumed that $(1 - c) \approx 1$ is a good approximation. The change of the concentration in time due to molecular and thermal diffusion is linked with the mass transport[3] by $\frac{\partial c}{\partial t} = -\frac{\vec{\nabla}\cdot\vec{j}}{\rho}$ in the case when convection is absent. The partial differential equation

$$\frac{\partial c}{\partial t} = D\vec{\nabla}\cdot\left[\vec{\nabla}c + S_T c(1-c)\vec{\nabla}T\right], \tag{2}$$

assuming a constant temperature gradient, can then be used for the description of the concentration's change in each of the two fluid reservoirs of the diffusion cell.[21] Völker and Odenbach[21] additionally assumed that the first term, related to the molecular diffusion, can be neglected due to its magnitude in comparison to the second term. Considering the fluid parameters given by Völker and Odenbach[21] the change in concentration is of the order of 10^{-2} of the homogeneous concentration of the dilute fluid (10^{-2}) over the cell's height of 10^{1} mm. The overall order of magnitude then results in $10^{-5}\ \mathrm{mm}^{-1}$. The second term with the Soret coefficient ($10^{-1}\ \mathrm{K}^{-1}$), the homogeneous concentration

and the temperature gradient (10^0 K/mm), then results in an order of magnitude of 10^{-3} mm^{-1} which is reasonably higher than the one of the therefore negligible first term. Furthermore, the concentration gradient is regarded constant and $\vec{\nabla} \cdot \vec{j}$ is substituted by $\left(\vec{j} \cdot \vec{n}\right) \frac{1}{l}$ due to the Gauss theorem. The direction of the mass flux is denoted $\vec{n}$ and l being the height of one fluid reservoir, perpendicular to the cross-section flown through by the mass flux. Völker and Odenbach[21] solved the resulting differential equation

$$\frac{dc}{dt} = -\frac{1}{l}\vec{n} \cdot \left(-DS_T c \vec{\nabla} T\right) \tag{3}$$

in one spatial dimension and separately for the two fluid reservoirs considering the mentioned assumptions and with $c(t=0) = c_0$ being the initial condition. The separation curve, being measured in the horizontal thermodiffusion cell, is then calculated as normalised difference of the concentrations of the lower (c_{lo}) and upper (c_{up}) reservoirs being

$$\frac{c_{lo} - c_{up}}{c_0} = \frac{2}{l} DS_T T_{,z} t \tag{4}$$

in a linear approximation with $T_{,z}$ denoting the temperature gradient in the z-direction. This approximation is only valid either for a relatively short separation time t, still being a couple of days long, or a small temperature gradient $T_{,z}$ which has to be considered while carrying out separation experiments. The separation time of the experimental detection of thermal diffusion divides the detected signal into a state when concentration changes are linear, as shown in Eq. (4), and a steady state. Both regimes contain information about the Soret coefficient but reaching the steady state of separation in a cell of a height of 0.01 m, takes about 50 to 60 days[9] due to the small diffusion coefficient of magnetic fluids in the order of 10^{-12} m^2/s. A higher cell then leads to an even longer time to reach this state, which makes it unaccessible for the experiments which are therefore carried out within the linear state. Some analytical and numerical investigations based on the above mentioned phenomenological approach and on the diffusion equation (2) have been done,[22–24] but there is still a lack of consistency between theoretical and experimental investigations in the horizontal thermodiffusion cell.

Besides this phenomenological description for dilute fluids, the ferrofluiddynamics-theory[19,20] has been developed on thermodynamic principles in a macroscopic consideration of the binary liquid. The mass flux

$$\frac{\vec{j}}{\rho} = -\xi \frac{\partial \mu_c}{\partial \rho_1} \vec{\nabla} c - \left(\frac{\xi_1}{\rho} + \frac{\xi}{\rho} \frac{\partial \mu_c}{\partial T}\right) \vec{\nabla} T \ , \tag{5}$$

with $\mu_c = \frac{k_B T}{m_1} ln \frac{\rho_1}{\rho} - \frac{k_B T}{m_2} ln \frac{\rho_2}{\rho} + const$ being the chemical potential, is described by the two Onsager parameters ξ and ξ_1.[19,20,25,26] The definition of these two is best done by the comparison with Eq. (1) or by a procedure analogue to the one described above to obtain a separation curve

$$\frac{c_{lo} - c_{up}}{c_0} = \frac{2}{l c_0 \rho} \left(\xi_1 + \xi \frac{\partial \mu_c}{\partial T}\right) T_{,z} t \ . \tag{6}$$

The derivatives of the chemical potential in this description are regarded as constant with the initial homogeneous concentration c_0 as governing concentration.

The experimental and theoretical investigations on thermodiffusion in magnetic fluids will be discussed in Secs. III–V starting first of all with the characterisation of the two concentrated magnetic fluids which provide relevant fluid parameters.

III. FLUID CHARACTERISATION

The experimental and theoretical work described in Secs. IV and V is based on the fluid parameters of two industrial ferrofluids provided by Ferrotec, the EMG905- and the APG513A-fluid. Both fluids contain magnetite particles, but the APG-fluid is an ester-based while the EMG-fluid is a kerosene-based ferrofluid. As already shortly mentioned in the introductory part, the diffusive

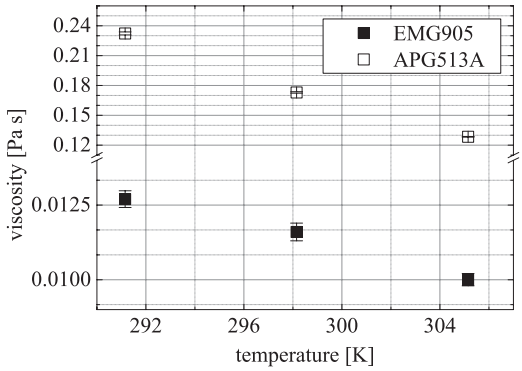

FIG. 1. Dynamic viscosity of the fluids APG513A and EMG905 in dependence on the temperature, measured at 291 K, 298 K, and 305 K. Reprinted with permission from L. Sprenger, A. Lange, and S. Odenbach, C. R. Mec. **341**, 429–437 (2013). Copyright 2013 Académie des sciences.

transport in a colloidal suspension is directly influenced by the fluid's viscosity, by the concentration, and the size of the dispersed particles. The dynamic viscosity η in this context is measured indirectly by determining the flow curves for the fluids[27] by measuring the shear stress τ in dependence on the shear rate $\dot{\gamma}$ with a shear-rate-controlled Anton Paar rheometer (Physica MCR301). Since ferrofluids in zero magnetic field and for low shear stress are expected to show Newtonian behaviour, the flow curve has a constant slope which represents the dynamic viscosity. The viscosity is exponentially dependent on the temperature[28] by $\eta = \eta_0 \exp(-E_A/(RT))$, with η_0 and E_A being fit parameters, and R is the universal gas constant. After having determined the thermodiffusion setup's average temperature, this dependence is used to calculate the average viscosity of the fluid under investigation. The viscosities for the two fluids at three different temperatures, relevant in the separation experiments, are plotted in Figure 1. The viscosity of the APG-fluid is one order of magnitude higher than the one of the EMG-fluid and the ferrofluids become more viscous with decreasing temperature.

To determine the particle's characteristics, magnetisation curves are detected by a vibrating sample magnetometer (VSM, Lakeshore). The magnetisation is plotted over the inner magnetic field of the ferrofluid sample and can be described by

$$M = \varphi M_d L(\xi_L) \tag{7}$$

with L being the Langevin function and $\xi_L = \frac{\mu_0 M_d V H}{k_B T}$ the Langevin parameter, M_d is the bulk magnetisation of the magnetic material (for magnetite: $M_d = 450$ kA/m), k_B is the Boltzmann constant, T is the temperature, V is the volume of one magnetic particle, and μ_0 is the vacuum permeability.[1] The volume concentration φ denotes the volumetric share of the sum of all magnetic

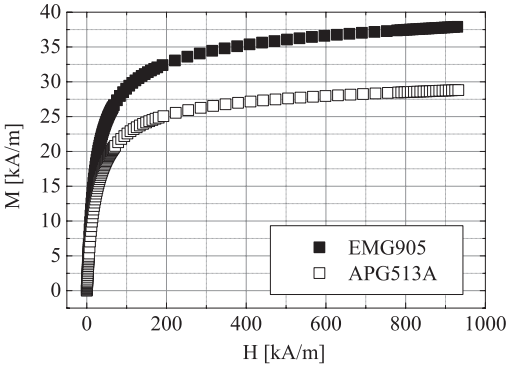

FIG. 2. Magnetisation of the APG513A- and the EMG905-fluid in dependence on the inner magnetic field at 291 K. Reprinted with permission from L. Sprenger, A. Lange, and S. Odenbach, C. R. Mec. **341**, 429–437 (2013). Copyright 2013 Académie des sciences.

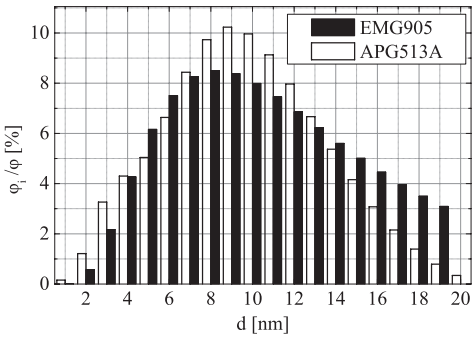

FIG. 3. Particle size distribution of the APG513A-fluid (Weser-method[30]) and the EMG905-fluid (Chantrell-method[31]).

particles in the entire fluid volume. Figure 2 shows the curves for both fluids. The magnetisation saturates for high magnetic field strengths which gives the opportunity to determine the volume concentration of the fluid by $M_s = \varphi M_d$, M_s denotes the saturation magnetisation.[1] The concentration of the APG-fluid is determined to 6.63 vol.% and for the EMG-fluid 8.67 vol.% is detected. The magnetisation in small magnetic fields increases linearly with the inner field strength so that a mean magnetic particle diameter can be calculated by the initial susceptibility

$$\chi_i = \frac{\pi \varphi \mu_0 M_d^2 d^3}{18 k_B T}, \tag{8}$$

which is the slope of the linear part of the curve.[1] Both fluids contain particles of a mean diameter of 11.5 nm. Since ferrofluids do not contain monodisperse particles, as supposed by the Langevin approach, a particle size distribution must be calculated by the regularisation method by Weser and Stierstadt.[30] A second method to determine the size distribution is offered by Chantrell *et al.*,[31] fitting the experimental magnetisation curve via a Langevin-function considering a lognormal distribution of the particles' size. Both methods rely on the VSM data and lead to weighed particle diameters of 10.4 nm in the EMG-fluid and 9.8 nm in the APG-fluid. The particle size distribution for both fluids is plotted in Figure 3. The APG's distribution is calculated by the Weser-method.[30] Since this method did not lead to physically consistent fluid parameters in the case of the EMG-fluid, the particle size distribution of the latter has been determined by using the Chantrell-method.[31]

The parameters mentioned have a direct impact on the diffusivity of the fluids characterised by the diffusion coefficient D. It is described by the Batchelor-corrected Einstein relation[32,33]

$$D = \frac{k_B T}{3\pi \eta_{CL}(d + 2s)}(1 + 1.45\varphi), \tag{9}$$

with $s = 2$ nm being a realistic surfactant layer thickness. The carrier liquid's viscosity η_{CL} can be derived from the ferrofluid's viscosity and its concentration by the relation $\eta = \eta_{CL}(1 + 2.5\varphi + 6.2\varphi^2)$ by Batchelor.[13] Magnetic particle interaction can be neglected in the diffusivity of this fluid since no magnetoviscous effect could be measured.[34] This leads to a diffusion coefficient of 3.9×10^{-12} m^2/s for the EMG-fluid and to 2.3×10^{-13} m^2/s for the APG-fluid at the experimental temperature of 298 K.[29]

IV. EXPERIMENTS ON THERMODIFFUSION

A. Experimental setup

Due to the advantages mentioned in Sec. II, a horizontal diffusion cell based on the design of Völker and Odenbach[21] is used to carry out the experiments on thermal diffusion. The setup includes the fluid container (1), 14 mm high and with an inner diameter of 10 mm, refer to Figure 4. It is axial-centrally separated into two reservoirs by a double-layer grid (2) reducing the actual separation chamber's height to 1 mm which is the distance between the two grids. Two independently controlled sensor coils (3) wrapped around the fluid reservoirs on both sides of the

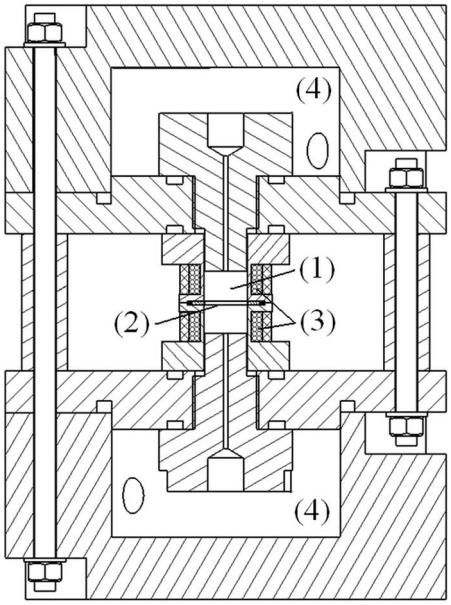

FIG. 4. Main components of the horizontal thermodiffusion cell: (1) fluid container, (2) double-layer grid, (3) sensor coils, and (4) tempering water baths. Reprinted with permission from L. Sprenger, A. Lange, and S. Odenbach, C. R. Mec. **341**, 429–437 (2013). Copyright 2013 Académie des sciences.

central grid detect the average concentration in each reservoir due to their inductance which is sensitive to the amount of magnetic material inside the coil. Each coil is 7 mm long and has an inner diameter of 12 mm. The inductance data are detected by a LCR measuring bridge (HP4284A) at a current of 10 mA, a voltage of 1 V, and a frequency of 10 kHz. Every minute a control program (Labview) reads out and stores the inductance and resistance signal of the upper and then with a delay of 10 s of the lower coil. The inductance of one coil ranges from 260 μH (empty) to 320 μH (filled with magnetic fluid), while the resistance is about 9 Ω. The temperature gradient is applied to the fluid container by two water baths (4) which are adjusted manually.[29]

The reduction of the separation chamber's height by the mentioned grid is, seen from the fluid mechanical point of view, not necessary in the following separation experiments. But since the same setup is also used in magnetic experiments, where convective motion can arise even in a thermally stable setup when not using the grid,[21] it is also used here for the reason of comparability, since it is a component being positioned within the diffusive mass flux. Its influence on the diffusive mass flux is discussed in Sec. IV B.

The accuracy of the measurement depends on several issues which are to a great deal temperature-related. Even the change of the environmental temperature during day-night-cycles can have an impact on the sensor coils and therefore on the measured data. To minimise that impact the main parts of the cell are made of a polymer which has an insulating effect. As far as the accuracy of the thermostats to heat and cool the water baths or the room temperature is concerned, experiments prior to the separation experiments have to investigate the actual temperature development in the fluid container under experimental circumstances. These experiments will be explained in detail in Sec. IV B. But the accuracy of the measured data is also dependent on the sensor coils' parameters detecting the concentration change by their change in inductance. To measure the inductance of a coil, the LCR measuring bridge sends a current impulse, which induces a magnetic field around the coil's windings. The area this field spans contains magnetic nanoparticles which are detected by a change in the inductance of the coil if they enter or leave this area. To get a very accurate measurement of the concentration in each fluid reservoir it needs to restrict the spreading of the magnetic field as far as possible to the geometry of the fluid reservoir itself. The spreading of the field is thereby correlated with the diameter of the coil. The intensity of the inductance signal is correlated with the number of the coil's windings. Since the inductances of the two coils are detected

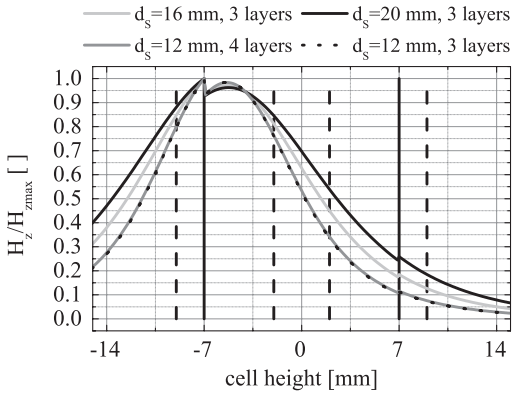

FIG. 5. Relative magnetic field strength of one sensor coil (dashed vertical lines) plotted over the fluid container's height (solid vertical lines) for different coil diameters and different numbers of winding layers.[35]

with a time shift of 10 s, numerical simulations done with Comsol Multiphysics Modelling only determine the axial component of the magnetic field strength of one coil with respect to the entire fluid container's height (14 mm), see Figure 5. The container's height is marked by the solid vertical lines, the first two dashed lines mark the position of the lower, the third and fourth of the upper sensor coil. The axial field strength is normalised by its maximum and the coil's diameter d is varied. The plot emphasises that the smaller the diameter the more distinct the field's maximum is and the faster the field strength decreases towards the coil's boundaries, indicated by dashed vertical lines. Therefore, a minimal diameter of 12 mm is chosen for the separation experiments. The number of winding layers increases the absolute inductance of the coil, but, once chosen the diameter, does not affect the normalised shape of the axial magnetic field strength. For that purpose, 4 layers are realised which is a reasonable number for a hand-wrapped coil. The wire used is a copper wire of a diameter of 0.2 mm.[35]

The separation experiments are always processed in exactly the same manner. While the fluid-cell is still empty the temperature gradient is applied and the coils' inductances are recorded at least until they are constant in time. In the next step, the cell is filled up and heated to the initial homogeneous temperature. The inductances are detected until a steady state is reached. After this the fluid container is exposed to the temperature gradient of 1 K/mm in the major part of the experiments and the inductances are determined for about 72 h. With the inductance data of the three phases, it is possible to calculate the change in the concentration between the two fluid reservoirs and the Soret coefficient according to Eq. (4). The accuracy of the value obtained in that way depends on the accuracy of the single parameters entering Eq. (4): $\Delta T = 13.5 \pm 0.5$ K, $\eta_{CL} = 8.70 \pm 0.25$ mPa s, $\varphi = 0.0867 \pm 0.0004$, and $l = 6.35 \pm 0.15$ mm. The resulting experimental error of the Soret coefficient is thereby determined to 0.015 K^{-1}.

B. Separation experiments

The thermodiffusion cell is first tested by detecting the temperature in the inside of the fluid container, when the temperature gradient is applied. Therefore, a fluid container is prepared with equally distanced thermistors (temperature-sensitive resistances) on one fluid reservoir instead of the sensor coil. There are three temperature sensors in the cross-section at a distance of 1.2 mm from the centre of the cell and at angles of 120° from each other (Fig. 6). There are two more sensors in the axial direction of the cylindrical container equally distanced 1.2 mm from each other and the other three thermistors (Fig. 6). With this setup, the temperature distribution in the fluid cell can be detected under the experiment's conditions. First a constant temperature of 298 K is established, followed by a temperature difference of 14 K over the container's height of 10 mm. Since the cell is only equipped with thermistors on one fluid reservoir, the same procedure is repeated after having turned around the cell. The temperature is plotted in Figure 7. It can be seen that fluctuations of the temperature on each cross-section appear due to the environmental temperature, but the

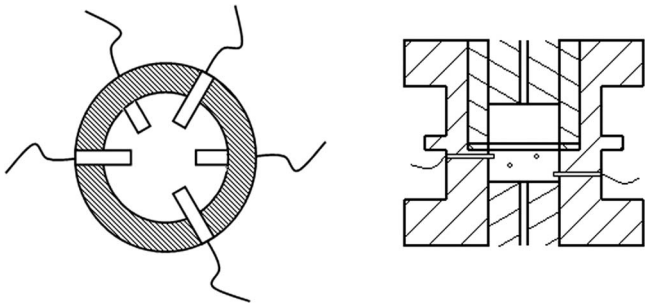

FIG. 6. Left: Cross section of the fluid container, including all temperature sensors with their azimuthal position. Right: Temperature sensors are shown regarding their axial position.

temperature gradient is mainly independent of the fluctuations, since these occur globally with respect to the entire diffusion cell. The error bars for the two central temperatures indicate the variation of the temperature between the three thermistors positioned in this cross section. It can be seen that the temperature distribution can be assumed constant at one height of the fluid cell, since the error is negligible. Fig. 8 emphasises the constant temperature distribution in the cross section close to the double-layer grid during the run of an entire experiment. Since the cross sectional temperature is constant as well in the limits of the environmental temperature as the positioning of the sensors, convective motion, possibly having an impact on the diffusive transport, can be excluded. An additional experiment detecting the middle temperature of the cell by a thermistor placed between the two grids leads to a middle temperature of 297.45 $\pm$ 0.15 K which is also constant in the range of the environmental temperature.

The next step is to find out about the fluids' characteristics in thermal diffusion that are important for accurate measuring data. For that purpose the two industrial ferrofluids already described in Sec. III and a third fluid, which is pure kerosene, are measured for separation. Figure 9 presents the change in the inductance of the lower and upper coil normalised with the initial inductance for these three fluids. The kerosene is measured to exclude the possibility that changes in the inductance are merely temperature-dependent. The ferrofluids show a very different behaviour of the inductance with a slope for the EMG905-fluid that is of one order of magnitude higher than for the APG513A-fluid. Since the magnetic parameters and even the structure of the fluids are similar, the difference in the signal detected is correlated with the viscosity, i.e., with the diffusivity of the fluid. The very high viscosity of the APG-fluid leads to a difference in the diffusion coefficient of one order of magnitude. Since the detectable absolute signal in the separation process of the EMG-fluid is higher, this fluid is chosen to perform the other separation experiments.

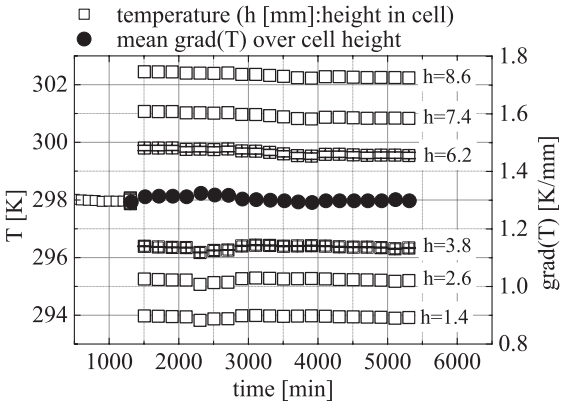

FIG. 7. Temperature profiles in a fluid container of the thermodiffusion cell with a height of 10 mm over the experimental time of 72 h, measured with a temperature difference of 14 K, heating the upper and cooling the lower wall.

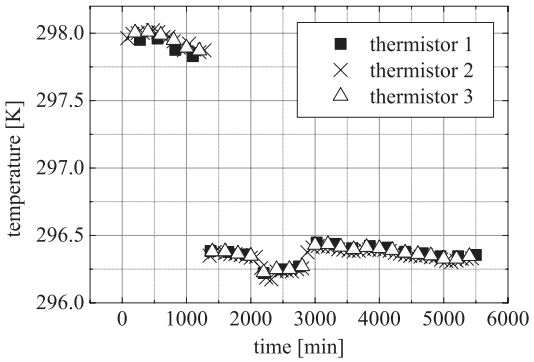

FIG. 8. Temperatures detected on the same cross section underneath the grid are compared with each other to exclude convective motion being present. Temperature changes along the time scale are due to changes in the environmental temperature.

To correctly process and interpret the measuring data, the dependence of the separation process on the temperature gradient has to be considered. Therefore, the EMG-fluid's separation is performed at three different temperature gradients and the arising concentration difference is plotted over the process time in Figure 10. The plot emphasises that a growing temperature gradient results in a higher inclination of the separation curve, as is already assumed by the mathematical description in Eq. (4). The linear dependence of the separation curve on the temperature gradient can also be proven. Since a gradient of 1 K/mm can still be realised in a fluid cell, 14 mm high, with reasonable effort of insulating the cell and a rather high coil response to separation, this gradient is chosen for all other experiments.

A last experimental comparison is carried out by recording the separation curve for two different grid materials, namely polyamide and brass. Since the grid is the only cell component located inside the diffusing fluid, it is important to know if different grid characteristics such as the heat conductivity have an impact on the separation curve. The two curves measured are plotted in Figure 11. A significant difference in the slope of both curves cannot be detected, this is why a significant impact of the grid inside the diffusive flux can be excluded.

All separation experiments can finally be used to calculate the Soret coefficient for the two fluids using Eq. (4) for dilute fluids and the experimental and fluid-related parameters. The Soret coefficient of the EMG-fluid is determined to $0.169 \pm 0.015\ \mathrm{K}^{-1}$, the coefficient of the APG-fluid is calculated to $0.219 \pm 0.015\ \mathrm{K}^{-1}$.

Since theoretical investigations standing alone cannot determine the Soret coefficient, the experimentally determined value for the EMG-fluid will be used to calculate the concentration profile

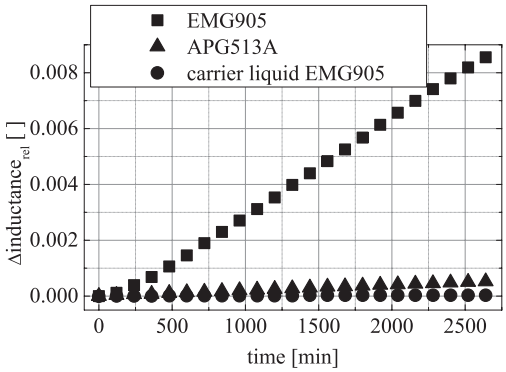

FIG. 9. Relative change in the inductance of the sensor coils of the measuring cell due to a temperature gradient of 1 K/mm which results in thermal diffusion measured for the EMG905-fluid, the APG513A-fluid, and pure kerosene. Reprinted with permission from L. Sprenger, A. Lange, and S. Odenbach, C. R. Mec. **341**, 429–437 (2013). Copyright 2013 Académie des sciences.

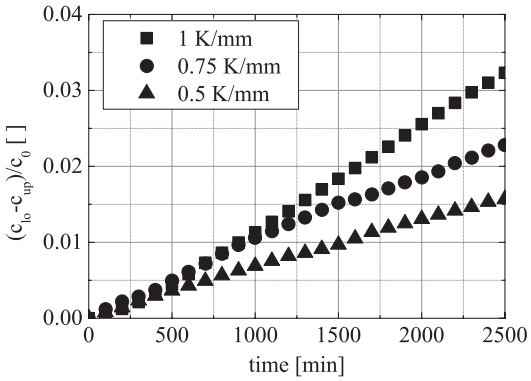

FIG. 10. Normalised concentration difference of the EMG905-fluid detected for three different temperature gradients: 0.5 K/mm, 0.75 K/mm, and 1 K/mm.

in Sec. V. The separation curve obtained in that way can be compared to the experimental one to validate as well the former as the theoretical *Ansätze* for the use with concentrated magnetic fluids.

V. THEORETICAL INVESTIGATIONS

A. Analytical investigations

Beside the theoretical investigations described in Sec. II, an analytical solution for the phenomenological diffusion equation (2) is calculated.[36] The method and solution used here can also be found in former works when investigating, for example, thermodiffusion in vertical columns.[37,38] In the case here it is assumed a one dimensional separation problem in a horizontal cell with the height h and a constant temperature gradient $T_{,z}$, still considering a dilute fluid $(1 - c \approx 1)$ due to restrictions in the analytical calculation, and a homogeneous initial concentration $c(z, t = 0) = c_0$. The boundaries of the cell are impermeable, means that the normal component of the mass flux is $j_z = -\rho D(c_{,z} + S_T c T_{,z}) = 0$ with $c_{,z}$ denoting the concentration gradient in the z-direction. The solution to the partial differential equation is obtained by a separation of the variables and reads

$$c(z,t) = C_0 e^{-Bz} + e^{-\frac{Bz}{2}} \sum_{n=1}^{\infty} e^{-k_n^2 t} C_n Y_n(z) \tag{10}$$

with

$$Y_n(z) = \frac{4\gamma_n - i2B}{B^2 + 4\gamma_n^2}[2\gamma_n \cos(\gamma_n z) - B \sin(\gamma_n z)], \tag{11}$$

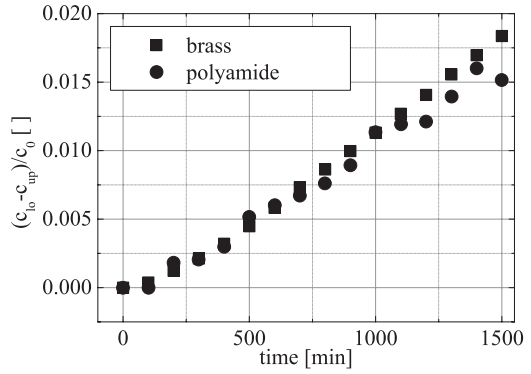

FIG. 11. Normalised concentration difference of the EMG905-fluid detected for grad$(T) = 1$ K/mm and two different grid materials: polyamide and brass.

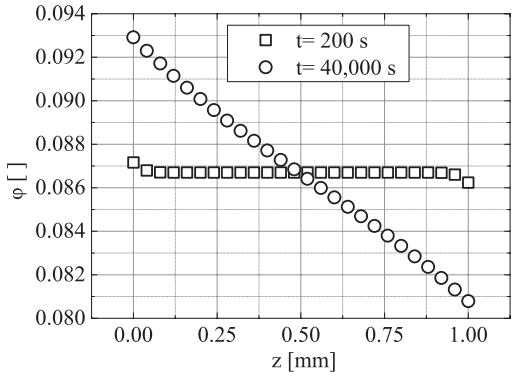

FIG. 12. The EMG-fluid's volume concentration is shown in dependence on the measuring-cell's height at two points in time: 200 s and 40 000 s. The concentration in the short time range piles up at the cell's boundaries, in the long range the concentration gradient becomes constant.

$$B = S_T T_{,z}, \tag{12}$$

$$C_0 = \frac{B c_0 h}{1 - e^{-Bh}}, \tag{13}$$

and

$$C_n = \frac{8 c_0 h B n \pi \left[(-1)^n e^{\frac{Bh}{2}} - 1\right](2n\pi + iBh)}{(4n^2\pi^2 - B^2h^2)^2 + 16B^2h^2n^2\pi^2}, \tag{14}$$

with $k_n^2 = D\left(\gamma_n^2 + \frac{B^2}{4}\right)$ and $\gamma_n = \frac{n\pi}{h}$. Two different cases can now be considered. The first one is a layer of fluid with a height of 1 mm and impermeable walls. This setup is adequate to study the general development of the concentration profile due to thermodiffusion, as can be seen in Figure 12 plotted for two different points in time. On the short time scale – 200 s – the separation of particles and fluid results in a piling up of concentration at the cell's boundaries. The separation process did not yet reach the middle part of the cell, where the homogeneous initial concentration remains unchanged. After a duration of the separation of 40 000 s, a constant concentration gradient can be calculated over the cell's height. Experimentally, the setup of a layer of only 1 mm of height cannot be realised. A point by point detection of the concentration over such a small gap using sensor coils as described in the experimental setup is impossible. To be able of carrying out a comparison between theoretical and experimental results, a second case analytically investigates the concentration development in a cell of a height of 14 mm as it is realised in the horizontal thermodiffusion cell. In the experiment the concentration is averaged over the fluid reservoirs positioned above and underneath the separation area. For the purpose of comparison the analytical concentration profile will be handled the same way, from $z = 0$ mm to $z = 6.5$ mm and from $z = 7.5$ mm to $z = 14$ mm the concentration is integrally averaged and a separation curve analogue to the one measured is calculated. Both separation curves, the analytical and experimental ones, are plotted in Figure 13. To fit the analytical data with the experimental separation curve for the concentrated fluid the Soret coefficient is varied from 0.184 K^{-1} to 0.154 K^{-1}, which is the span of the coefficient's value considering the experimental error. The most adequate fit between the two curves is obtained by the analytical separation curve assuming a Soret coefficient of 0.184 K^{-1} while the coefficient calculated via Eq. (4) is 0.169 K^{-1}. This difference can be related back to the assumptions made for the two *Ansätze*. Both approaches deal with dilute fluids ($1 - c \approx 1$), but Eq. (4) by Völker and Odenbach[21] additionally assumes a constant concentration gradient ($\vec{\nabla} c \approx$ const.) in the fluid reservoir and a negligible molecular diffusion ($\vec{\nabla} \cdot \vec{\nabla} c \approx 0$). The first assumption leaves out the boundary layers of the concentration profile that can be calculated via the analytical solution. The second assumption is only valid for small

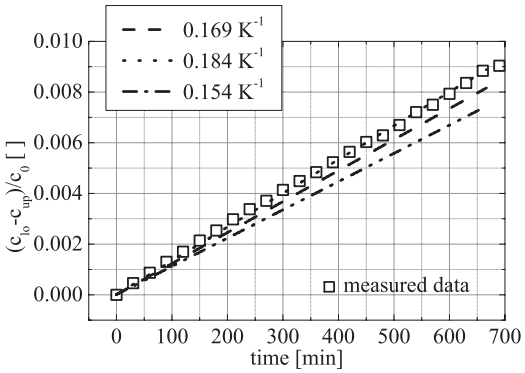

FIG. 13. Separation signal detected in the EMG905-fluid for grad(T) = 1 K/mm and compared with an analytically determined separation curve based on Eq. (10) for three different Soret coefficients: 0.154 K^{-1}, 0.169 K^{-1}, and 0.184 K^{-1}. The last one fits best the experimental data.

concentrations. The separation process is thereby underestimated in the case of a more concentrated magnetic fluid.

B. Numerical investigations

Numerical investigations involve the solution for the diffusion equation (5) based on the finite differences method (FDM). The time derivative is here defined by the Euler backwards scheme, the spatial derivatives are realised by the central differences scheme. The boundary conditions are either implemented by the forward- or backward-differences. The solution is calculated in three dimensions within the cylindrically shaped fluid cell. The grid knots in the axial direction z are equally distanced, the circular cross-section is divided into five different blocks, a Cartesian one, centrally placed, and four blocks, each 90° wide, surrounding the middle block. The time steps are kept constant during the numerical calculations.

Figure 14 compares the concentration profile over the separation layer of a height of 1 mm for two different points in time – 200 s and 40 000 s – and the analytical and numerical calculations. While the analytical solution is valid for dilute fluids only ($1 - c \approx 1$), the numerical one considers the term $1 - c = 1 - c_0$. For less concentrated magnetic fluids the analytical and numerical results are expected to be similar with a rising difference when the fluid's concentration rises.

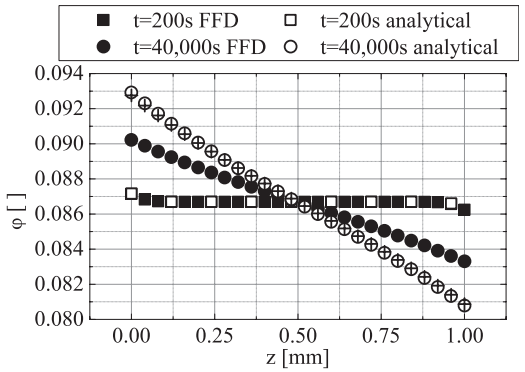

FIG. 14. The EMG-fluid's volume concentration is shown in dependence on the measuring-cell's height for $S_T = 0.169$ K^{-1} and grad(T) = 1 K/mm at two points in time: 200 s and 40 000 s. The concentration calculated via the FFD-theory is equal to the analytical solution in the short time range, but considerably smaller in the long range. The crosses represent the FFD-solution for $S_T = 0.29$ K^{-1}.

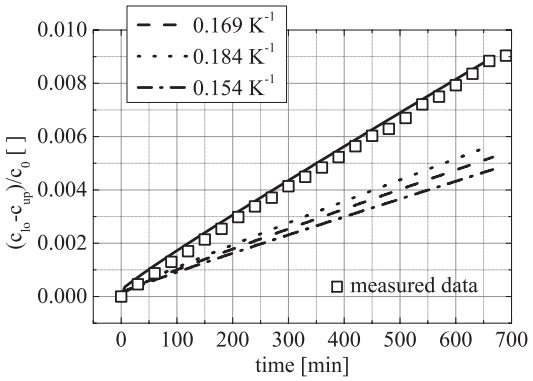

FIG. 15. Separation signal detected in the EMG905-fluid for grad(T) = 1 K/mm and compared with an analytically determined separation curve based on Eq. (10) for three different Soret coefficients (dashed lines): 0.154 K^{-1}, 0.169 K^{-1}, and 0.184 K^{-1}. The solid line represents the numerical separation curve calculated with a Soret coefficient of 0.29 K^{-1}.

Numerics are based on the following parameters: $\xi = 1.927 \times 10^{-13}$ kg s/m^3 and $\xi_1 = 3.033 \times 10^{-10}$ kg/(m s K). The numerically determined concentration for both time ranges in Figure 14 is smaller than the analytically calculated one, while the difference between the two solutions becomes wider in time. The crosses represent the numerically calculated concentration profile for a Soret coefficient of 0.29 K^{-1} and lead to a good fit with the analytical profile. This underestimation of the separation process by the analysis via Eq. (4) is also clearly visible in Figure 15. The measured data (cell's height: 14 mm) is compared with the numerically determined separation curves for three different Soret coefficient (0.169 K^{-1}, 0.184 K^{-1}, and 0.154 K^{-1}). None of these curves is able of fitting the experimental curve. While carrying out the numerical calculations with $S_T = 0.29$ K^{-1} (solid line in Figure 15) leads to a good agreement of numerical and experimental separation data.

Using the analytical and numerical calculation for a fluid less concentrated, e.g., the kerosene-based fluid of the work of Völker and Odenbach,[21] leads to Figure 16. The fluid contains magnetite nanoparticles distributed in kerosene. The volume concentration is about $\varphi = 0.02$ and the particles' diameter $d = 9$ nm. The diffusivity, characterised by the diffusion coefficient, is mentioned to be $D = 2 \times 10^{-11}$ m^2/s. It can be pointed out that the difference between the analytical and numerical concentration distributions is smaller than in the previous case of Figure 14 with a fluid 4.5 times higher concentrated, so that accuracy of the different analysing methods highly depends on the concentration of the fluid under investigation.

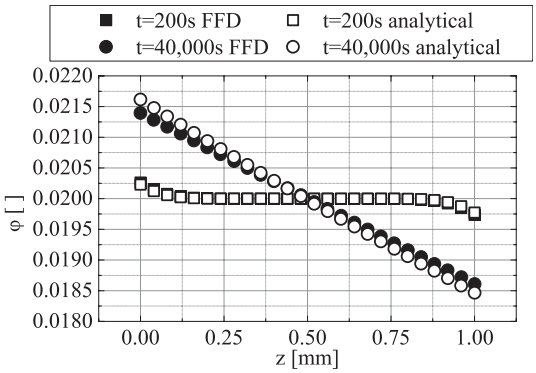

FIG. 16. The volume concentration of a dilute magnetic fluid ($\varphi = 0.02$, magnetite particles, kerosene-based carrier liquid) is shown in dependence on the measuring-cell's height for $S_T = 0.16$ K^{-1} and grad(T) = 1 K/mm at two points in time: 200 s and 40 000 s. Data are calculated via FFD-theory numerically ($\xi = 1.063 \times 10^{-12}$ kg s/m^3 and $\xi_1 = 2.892 \times 10^{-10}$ kg/(m s K)) and via an analytical solution.[36]

VI. RESULTS AND DISCUSSION

The aim of this review on thermodiffusion and the additional experimental and theoretical investigations is to apply previous results in that field to the concentrated fluids under investigation, and to compare and complement them with new experimental, analytical, and numerical results in the present work. The experiments on the thermodiffusive processes are carried out with a horizontal thermodiffusion cell and a kerosene-based magnetic fluid (EMG905) composed of magnetic nanoparticles with a volume concentration of 8.67 vol.%. Analysing the experimentally detected separation curves by the means of the previous works, $\frac{c_{lo}-c_{up}}{c_0} = \frac{2}{l} D S_T T_{,z} t$, the Soret coefficient is determined to $0.169 \pm 0.015\ \mathrm{K}^{-1}$, which is in the range of previous values for low-concentrated fluids. But since a dilute fluid is assumed in the diffusion equation $\frac{\partial c}{\partial t} = D\vec{\nabla} \cdot \left[\vec{\nabla} c + S_T c(1-c)\vec{\nabla} T\right]$ with $(1 - c) \approx 1$, the mass concentration c and the volume concentration φ do not need to be distinguished in this approach. Considering the fact that the density of the nanoparticles ρ_p is about 5 times higher than the carrier liquid's density ρ_{CL} and converting the mass into the volume concentration by $c = \varphi \frac{\rho_p}{\rho_{CL}}$ points out that in the special case of concentrated ferrofluids the two different definitions of the concentration have to be taken into account when solving the diffusion equation including the quadratic term $D S_T \vec{\nabla} \cdot (c(1-c)\vec{\nabla} T)$.

Besides the assumption of the fluid being dilute, the phenomenological approach of the previous work[21] also assumes a constant concentration gradient over the separation layer which leads, as mentioned to a Soret coefficient of $0.169\ \mathrm{K}^{-1}$. The coefficient is calculated to $0.184\ \mathrm{K}^{-1}$ for the analytical solution of the concentration development in the cell. Equation (10), describing the concentration profile in the fluid layer, is also based on the assumption of a dilute fluid $(1 - c) \approx 1$ but the concentration gradient over the layer is not assumed constant for the entire separation process and the molecular diffusion is not neglected as is possible when dealing with very low concentrations in the magnetic fluids. The numerical determination of the Soret coefficient via the experimental separation curve leads to $0.29\ \mathrm{K}^{-1}$. This *Ansatz* does not consider a dilute fluid and uses $1 - c = 1 - c_0$ as an approximation for the quadratic term in the diffusion equation, the concentration gradient as in the analytical solution is not considered constant and molecular diffusion is not neglected. The comparison of the three differently calculated Soret coefficients points out that approaches for solving the diffusion equation considering a dilute fluid underestimate the intensity of the separation process in concentrated magnetic fluids, in the present case approximately by a factor of 2.

The horizontal thermodiffusion cell can be reliably used to detect separation curves of ferrofluids. The double-layer grid positioned in the measuring cell's centre does not influence the separation of nanoparticles and carrier liquid, although it induces irregularities in the temperature distribution by material parameters, such as heat conductivity, different from the fluid's parameters. The accuracy of the Soret coefficient's determination in concentrated magnetic fluids from the separation signal can be improved, in comparison to previous works mainly focussing on dilute fluids.

ACKNOWLEDGMENTS

The authors especially thank Professor Blums and Professor Zubarev for very helpful discussions. The financial support by the Deutsche Forschungsgemeinschaft in project LA 1182/3 is gratefully acknowledged.

[1] R. E. Rosensweig, *Ferrohydrodynamics* (Dover Publications, Mineola, NY, 1997).
[2] S. Odenbach, *Magnetoviscous Effects in Ferrofluids* (Springer-Verlag, Berlin, 2002).
[3] S. de Groot and P. Mazur, *Non-Equilibrium Thermodynamics* (North-Holland Publishing Company, Amsterdam, 1962).
[4] A. Mezulis, E. Blums, G. Kronkalns, and M. Maiorov, "Measurements of thermodiffusion of nanoparticles in magnetic colloids," Latv. J. Phys. Tech. Sci. **5**, 1–13 (1995).
[5] K. I. Morozov, "Thermodiffusion in magnetic colloids," J. Magn. Magn. Mater. **201**, 248–251 (1999).
[6] S. Odenbach, *Handbook of Magnetic Materials*, edited by K. H. J. Buschow (Elsevier, North-Holland Publishing Company, Amsterdam, 2006).
[7] C. Soret, "Sur l'état d'équilibre que prend, au point de vue sa concentration, une dissolution saline primitivement homogène, dont deux parties sont portées a des température différentes," Arch. Genève **3e periode, t. II**, 48 (1879).
[8] C. Ludwig, "Diffusion zwischen ungleich erwärmten Orten gleich zusammengesetzter Lösungen," in *Sitzungsberichte der kaiserl. Akad. d. Wissenschaften, mathemat.-naturwissenschaftl. Classe, XX* (K. K. Hof- und Staatsdruckerei, 1856).

[9] T. Völker, E. Blums, and S. Odenbach, "Thermodiffusion in magnetic fluids," J. Magn. Magn. Mater. **252**, 218–220 (2002).
[10] W. Köhler and B. Müller, "Soret and mass diffusion coefficients of toluene/n-hexane mixtures," J. Chem. Phys. **103**, 4367–4370 (1995).
[11] J. K. Platten, M. M. Bou-Ali, P. Costesèque, J. F. Dutrieux, W. Köhler, C. Leppla, S. Wiegand, and G. Wittko, "Benchmark values for the Soret, thermal diffusion and diffusion coefficient of three binary organic liquid mixtures," Philos. Mag. **83**, 1965–1971 (2003).
[12] B. Berkovsky and V. Bashtovoy, *Magnetic Fluids and Application Handbook* (Begell House, Inc., Redding, CT, 1996).
[13] G. K. Batchelor, "The effect of Brownian motion on the bulk stress in a suspension of spherical particles," J. Fluid Mech. **83**, 97–117 (1977).
[14] J. Philip, P. D. Shima, and B. Raj, "Evidence for enhanced thermal conduction through percolating structures in nanofluids," Nanotechnology **19**, 305706 (2008).
[15] J.-C. Bacri, A. Cebers, A. Bourdon, G. Demouchy, B. M. Heegaard, and R. Perzynski, "Forced Rayleigh experiment in a magnetic fluid," Phys. Rev. Lett. **74**, 5032–5036 (1995).
[16] J. Lenglet, A. Bourdon, J.-C. Bacri, and G. Demouchy, "Thermodiffusion in magnetic colloids evidenced and studied by forced Rayleigh scattering experiments," Phys. Rev. E **65**, 031408 (2002).
[17] E. Blums, S. Odenbach, A. Mezulis, and M. Maiorov, "Soret coefficient of nanoparticles in ferrofluids in the presence of a magnetic field," Phys. Fluids **10**, 2155–2163 (1998).
[18] T. Völker and S. Odenbach, "Thermodiffusion in magnetic fluids," J. Magn. Magn. Mater. **289**, 289–291 (2005).
[19] H. W. Müller and M. Liu, "Structure of ferrofluid dynamics," Phys. Rev. E **64**, 061405 (2001).
[20] A. Lange, "Magnetic Soret effect: Application of the ferrofluid dynamics theory," Phys. Rev. E **70**, 046308 (2004).
[21] T. Voelker and S. Odenbach, "Thermodiffusion in ferrofluids in the presence of a magnetic field," Phys. Fluids **17**, 037104 (2005).
[22] E. Blums, "Mass transfer in nonisothermal ferrocolloids under the effect of a magnetic field," J. Magn. Magn. Mater. **201**, 242–247 (1999).
[23] R. Savino and D. Paterna, "Thermodiffusion in nanofluids under different gravity conditions," Phys. Fluids **20**, 017101 (2008).
[24] R. Piazza and A. Parola, "Thermophoresis in colloidal suspensions," J. Phys.: Condens. Matter **20**, 1–18 (2008).
[25] L. Onsager, "Reciprocal relations and irreversible processes I," Phys. Rev. **37**, 405–426 (1931).
[26] L. Onsager, "Reciprocal relations in irreversible processes II," Phys. Rev. **38**, 2265–2279 (1931).
[27] F. A. Morrison, *Understanding Rheology* (Oxford University Press, New York, 2001).
[28] H. Fukuyama and Y. Waseda, *High-Temperature Measurements of Materials* (Springer-Verlag, Berlin, 2009).
[29] L. Sprenger, A. Lange, and S. Odenbach, "Thermodiffusion in ferrofluids regarding thermomagnetic convection," C. R. Mec. **341**, 429–437 (2013).
[30] T. Weser and K. Stierstadt, "Discrete particle size distribution in ferrofluids," Z. Phys. B: Condens. Matter **59**, 253–256 (1985).
[31] R. W. Chantrell, J. Popplewell, and S. W. Charles, "Measurements of particle size distribution parameters in ferrofluids," IEEE Trans. Magn. **14**, 975–977 (1978).
[32] A. Einstein, "Über die von der molekularkinetischen Theorie der Wärme geforderte Bewegung von in ruhenden Flüssigkeiten suspendierten Teilchen," Ann. Phys. **322**, 549–560 (1905).
[33] G. K. Batchelor, "Brownian diffusion of particles with hydrodynamic interaction," J. Fluid Mech. **74**, 1–29 (1976).
[34] H. Engler, "Parametric modulation of thermomagnetic convection in ferrofluids (in German)," Ph.D. thesis (TU Dresden, 2010).
[35] L. Sprenger, A. Lange, and S. Odenbach, "Influence of thermodiffusive particle transport on thermomagnetic convection in magnetic fluids," Magnetohydrodynamics **49**, 473–478 (2013).
[36] A. Zubarev and A. Lange, personal communication (2010).
[37] E. Blums, Y. A. Mikhailov, and R. Ozols, *Heat and Mass Transfer in MHD Flows* (World Scientific Publishing, Singapore, 1987).
[38] E. Blums and S. Odenbach, "Dynamics of thermodiffusive separation of ferrocolloids in vertical columns: the effect of solutale buoyancy," Magnetohydrodynamics **37**, 187–194 (2001).